Journal of Macromolecular Science, Part A
Publication details, including instructions for authors and subscription information:
http://www.informaworld.com/smpp/title~content=t713597274

The Use of Sodium Hydroxide Hydrolysis to Study the Fine Structure of Undrawn and Drawn High-Speed Spun Polyethylene Terephthalate) Fibers

S. A. Holmes[ab]; S. H. Zeronian[a]
[a] Division of Textiles and Clothing, University of California Davis, Davis, California [b] Division of Textiles, Apparel and Interior Design, The University of Texas at Austin, Austin, Texas

To cite this Article Holmes, S. A. and Zeronian, S. H.(1994) 'The Use of Sodium Hydroxide Hydrolysis to Study the Fine Structure of Undrawn and Drawn High-Speed Spun Polyethylene Terephthalate) Fibers', Journal of Macromolecular Science, Part A, 31: 9, 1147 — 1168
To link to this Article: DOI: 10.1080/10601329409351542
URL: http://dx.doi.org/10.1080/10601329409351542

J.M.S.—PURE APPL. CHEM., A31(9), pp. 1147–1168 (1994)

THE USE OF SODIUM HYDROXIDE HYDROLYSIS TO STUDY THE FINE STRUCTURE OF UNDRAWN AND DRAWN HIGH-SPEED SPUN POLY(ETHYLENE TEREPHTHALATE) FIBERS

S. A. HOLMES† and S. H. ZERONIAN*

Division of Textiles and Clothing
University of California, Davis
Davis, California 95616

ABSTRACT

The fine structures of undrawn and drawn high-speed spun poly(ethylene terephthalate) (PET) fibers, 0.86 dL/g intrinsic viscosity, formed at speeds from 1615 to 3329 m/min, were investigated. Increasing the spinning speed and drawing resulted in greater levels of orientation and crystallinity in the untreated fibers. The relatively high molecular weight of the PET yielded undrawn products of higher orientation and crystallinity than those obtained by workers using PET of lower molecular weight but spun at similar speeds. A linear relationship between cohesive and optical anisotropy was found for the undrawn and drawn fibers. Aqueous sodium hydroxide hydrolysis was utilized to reveal the presence of any radial variations in structure. In the undrawn fibers, hydrolysis revealed that a more oriented layer was present very near the fiber periphery at higher spinning speeds. In the drawn samples a small but significant progressive decrease in birefringence was generally observed as the center of the fiber was approached. The drawing process appears to produce fibers without a skin–core structure and less susceptible to tenacity loss due to surface defects.

†Present address: Division of Textiles, Apparel and Interior Design, The University of Texas at Austin, Austin, Texas 78712.

INTRODUCTION

High-speed spinning, with or without integrated drawing, is a relatively new one-step method for commercially producing poly(ethylene terephthalate) (PET) fibers. Many studies of undrawn high-speed spun PET fibers have appeared in the literature [1–8], but the structure of drawn high-speed spun PET fibers does not appear to have been reported. Some workers have found evidence of a skin–core type of structure in undrawn high-speed spun PET fibers [1–3]. This radially inhomogeneous structure is reported to appear at different speeds. Mukhopadhyay and coworkers [1] found a skin–core structure at a spinning speed of 6000 m/min, Shimizu et al. [2] did not detect such a structure until 9000 m/min, and the PET fibers studied by Vassilatos et al. [3] showed radial variations in birefringence as early as 3111 m/min. In addition to spinning speed, other parameters were varied, and this may contribute to the differences in the results of the cited studies. Distributions of temperature and stress across the fiber due to rapid quenching during spinning and an increase in the orientation-induced crystallization rate have been cited as reasons for the development of a skin-core structure [2].

Aqueous sodium hydroxide hydrolysis has been shown to be a useful tool for examining the fine structure of PET fibers [9]. As described in a review article [10a], many studies have concluded that hydrolysis occurs only at the PET surface; the remainder of the fiber is not affected. Confirming evidence can be found in articles published since the review article. The molecular weight distribution of PET fiber has been found to remain virtually unaffected as the fiber is hydrolyzed with aqueous sodium hydroxide up to a weight loss of 91% [9]. Any tenacity loss of the hydrolyzed fiber is therefore not related to its degree of polymerization. In fact, tenacity reduction at low weight losses (up to 30%) is very small, and the decrease in tenacity at higher weight losses has been explained in terms of initiation of failure at surface defects [9, 18]. In contrast, aminolysis, a permeant reaction, causes major changes in the molecular weight distribution of PET fiber as the degree of polymerization decreases. The relation between the tenacity of aminolyzed fibers and their number-average molecular weight is linear [10b]. In other work the kinetics of PET dissolution in aqueous sodium hydroxide has been described by a model in which the reaction occurs at the fiber surface [10c]. Also, the radii of caustic-treated PET fibers calculated from the initial radius of the fiber and the weight loss agree closely with measured radii [9]. Thus, successive layers of PET fiber can be removed by aqueous sodium hydroxide, allowing study of the fine structure at various depths into the fiber.

This study had two objectives: 1) to investigate the fine structure of high-speed spun PET fibers before and after drawing, and 2) to utilize aqueous NaOH hydrolysis to reveal radial differences in the fine structure of undrawn and drawn high-speed spun PET fibers.

EXPERIMENTAL

Materials

High-speed spun delustered PET yarns were provided by Hoechst Celanese, Charlotte, North Carolina. A total of eight samples were studied; four of the yarns were spun at speeds ranging from 1615 to 3329 m/min and left undrawn, while the

remaining four yarns were counterparts which had been drawn subsequently. The sample codes together with the spinning and drawing conditions are given in Table 1. All chemicals used were of reagent grade.

Procedures

Alkaline Hydrolysis. All hydrolyses were carried out in sealed flasks at 21°C (± 2°C) with mild mechanical agitation. Yarn samples were treated in a 2.5 M aqueous NaOH, 0.1% (w/w) cetyltrimethylammonium bromide (CTAB) solution in a 2.5 ratio of weight/volume (g/L) for various lengths of time. CTAB was used to increase the rate of the reaction. The hydrolysis termination and sample rinsing and drying were performed in the manner described previously [9].

Weight Loss. The percentage weight loss was determined after the hydrolyzed samples had been conditioned by coming to constant weight at 21°C (± 2°C) and 65% relative humidity. It was calculated based on the conditioned weight of the untreated samples.

Scanning Electron Microscopy. Samples were mounted on standard specimen stubs with silver paint and then coated with gold. Photomicrographs were taken using an International Scientific Instruments Model DS 130 microscope operating in the secondary mode at an accelerating voltage of 10 kV.

Birefringence. Birefringence (Δn) was measured by the Becke line method. Fibers were immersed in liquids of known refractive index (R. P. Cargille Laboratories, Inc.) and viewed under a Zeiss polarizing light microscope. Adjacent sections of the same fiber were used to obtain the refractive indices parallel to ($n_{\parallel}$) and perpendicular to ($n_{\perp}$) the fiber axis, and Δn was then calculated by

TABLE 1. Spinning and Drawing Conditions of the Untreated PET Fibers

Sample code	Spinning speed, m/min	Draw ratio	Tex[a]
Undrawn:			
U1	1615	—	0.726
U2	2162	—	0.735
U3	2553	—	0.733
U4	3329	—	0.722
Drawn:			
D1	1615	2.44	0.357
D2	2162	2.10	0.363
D3	2553	2.04	0.354
D4	3329	1.88	0.363

[a]Tex is the weight in grams of 1 kilometer of filament.

$$\Delta n = n_{\parallel} - n_{\perp}$$

The birefringence of 10 fibers was measured and averaged.

Density. Measurements were made at 21°C (± 2°C) in a density gradient column prepared with carbon tetrachloride and *n*-heptane.

Intrinsic Viscosity. The relative viscosity was measured in a 4% (w/v) solution of phenol/1,1,2,2-tetrachloroethane (3/2 v/v) at 25°C (± 0.1°C). The intrinsic viscosity was calculated using a one point method according to Billmeyer's equation [11]:

$$[\eta] = 0.25\eta_{sp}/c + 0.75 \ln \eta_r/c$$

where $[\eta]$, η_{sp}, η_r, and c are the intrinsic viscosity in dL/g, the specific viscosity, the relative viscosity, and the solution concentration in g/dL, respectively. The molecular weight was calculated using the Mark-Houwink equation [12]:

$$[\eta] = KM_v^a$$

where $K = 7.44 \times 10^{-4}$ dL/g and $a = 0.648$ [13].

Tensile Strength. Single fiber breaking loads were measured using a table model Instron Universal Testing Machine with a 2.54 cm gauge length at 2 cm/min constant rate of elongation at 21°C(± 2°C) and 65% relative humidity. The results are the average of 25 tests.

Tex. Three 1-meter lengths of the untreated yarn were conditioned at 21°C (± 2°C) and 65% relative humidity and weighed. The average weight was divided by the average number of fibers in the yarn and multiplied by 1000 to obtain the text of the untreated fiber. The tex of the hydrolyzed fibers was calculated using the percentage weight loss.

Initial Modulus. The initial modulus was measured by determining the slope of the initial linear portion of the stress-strain curve obtained from the fiber tensile tests.

Torsional Modulus. Essentially, Meredith's torsion pendulum method [14], in which a fiber is freely suspended with an inertia bar attached to the free end, was used to measure the fiber torsional modulus (TM), calculated as

$$\mathrm{TM} = 8\pi^3 IL/T^2S^2\epsilon \tag{1}$$

where I is the moment of inertia of the bar in g·cm^2, L is the free length of the fiber in cm, T is the true period of oscillation in seconds, S is the cross-sectional area of the fiber in cm^2, and ϵ is a shape factor equal to 1 for fibers with circular cross-sections such as PET. Damping is accounted for by calculating T from the observed period of oscillation, T_0:

$$T = T_0/\sqrt{1 + (\lambda/2\pi)^2} \tag{2}$$

where λ is the logarithmic decrement, given by

$$\lambda = \ln A_1/A_2 \tag{3}$$

A_1 and A_2 are the times of two successive swings of the pendulum in the same direction.

Expressing S in Eq. (1) in terms of fiber diameter, d, gives

$$S = \pi d^2/4 \tag{4}$$

Substituting Eq. (4) into Eq. (1) gives

$$\mathrm{TM} = 128\pi IL/T^2d^4 \tag{5}$$

All measurements were made at 21°C (± 2°C) and 65% relative humidity. The results are the average of nine determinations.

Diameter. For purposes of calculating the initial and torsional moduli, the fiber cross-sectional area was obtained from the fiber diameter, measured using light microscopy. Fibers were immersed in glycerol and viewed at a magnification of 400 using a Nikon binocular microscope fitted with a calibrated eyepiece. For all but the highest weight loss samples, the diameter of 10 fibers was measured and averaged. Due to the larger variation in diameter at high weight loss and the dependence of TM on the reciprocal of the diameter raised to the fourth power, the diameter of the same fiber used to measure TM was measured and used in calculations rather than the average of 10 separate fibers.

RESULTS and DISCUSSION

Untreated Fibers

All samples were produced using a one-step method with drawing integrated into the spinning line. The intrinsic viscosity of the fibers was 0.86 dL/g, corresponding to $M_v = 53{,}300$.

Orientation

As spinning speed increased, the orientation of the undrawn untreated fibers, as indicated by their birefringence, increased significantly (Table 2). This effect was due to the additional stress placed on the spinning line as speed increased. After drawing, spinning speed was virtually irrelevant, although the fibers were drawn to different draw ratios (Table 1). Nevertheless, the fact that drawing the least oriented undrawn sample, U1, to a ratio only slightly greater than that of the most oriented undrawn sample, U4, resulted in approximately the same level of orientation is indicative of the ease of deformation of fibers spun at slow speeds. In their attempt to produce a PET fiber with the greatest possible birefringence, Gupta et al. [4] found that drawing and heat-setting of a fiber spun at a slow speed (1000 m/min) had a higher birefringence than a drawn and heat-set fiber spun at either 3000 or 5500 m/min, which they claimed was due to the greater deformability of the slowly spun fiber.

The birefringence values of the undrawn fibers investigated herein are greater than those reported in other studies of PET fibers spun in the same speed range [5, 6]. Those studies described the effects of molecular weight on various properties of

TABLE 2. Selected Physical Properties of Untreated PET Fibers

Sample	Birefringence	Density, g/cm^3	Tenacity, g/tex	TM,[a] GPa	IM/TM[b]
U1	0.030	1.343	22.3	0.65	3.05
U2	0.048	1.348	27.7	0.66	4.44
U3	0.064	1.358	30.4	0.65	4.77
U4	0.088	1.371	31.0	0.72	6.14
D1	0.181	1.397	69.1	0.85	10.36
D2	0.182	1.394	73.6	0.77	12.49
D3	0.186	1.399	78.3	0.85	12.48
D4	0.186	1.401	78.1	0.88	12.85

[a]TM = torsional modulus.
[b]IM = initial modulus.

PET fibers spun at several speeds. Chen et al. [5] compared PET fibers of M_v = 15,700 and 28,700. The PET fibers used by Shimizu et al. [6] were of M_v = 18,400, 20,500, and 29,800. Both groups of researchers found an increase in birefringence with molecular weight. Comparing fibers spun at approximately the same speed, the birefringence of all fibers used in the two cited studies [5, 6], regardless of molecular weight, was lower than that of the fibers used in the present work. For instance, the fibers used by Chen et al. [5] spun at 3000 m/min had birefringence values of approximately 0.035 and 0.050 for the lower and higher molecular weights, respectively. The birefringence of any of the three samples spun at 3000 m/min by Shimizu et al. [6] did not exceed approximately 0.030. In contrast, our sample, spun at 3329 m/min, had a birefringence of 0.088, which is nearly twice that of the other researchers' samples. In another study of the effects of molecular weight, Heuvel and Huisman [7] reported that increasing the specific viscosity of the polymer by 0.1 had the same effects as increasing the spinning speed by 500 m/min. Therefore, it appears that the relatively high molecular weight (M_v = 53,300) of the undrawn samples used in this study is the reason for their greater orientation than those of previously examined PET fibers spun at comparable speeds.

Crystallinity

The crystallinity of the undrawn samples as indicated by density measurements increased significantly with spinning speed while the drawing process crystallized the undrawn samples to nearly equal extents, regardless of spinning speed (Table 2). The undrawn sample spun at 1615 m/min (Sample U1) had a density of 1.343 g/cm^3, not much greater than that of completely amorphous PET which has a density of 1.335 g/cm^3 [15].

Compared to other results found in the literature, as with the birefringence measurements, the density of the undrawn samples was greater than that of other high-speed spun PET fibers. Chen et al. [5] did not observe the development of "significant" crystallinity until a spinning speed of 3000 m/min for their sample of

M_v = 28,700 or 4000 m/min for PET of M_v = 15,700. This significant level of crystallinity was present in Sample U1 of this study, spun at only 1615 m/min with M_v = 53,300. Heuvel and Huisman [7] studied PET fibers of different viscosities spun at various speeds and found the density of all three samples spun at 3000 m/min to be in the range of 1.340 to 1.343 g/cm^3. This is approximately equal to the density of Sample U1 (Table 2), spun at 1615 m/min with an intrinsic viscosity of 0.86 dL/g. We calculate that the intrinsic viscosities of Heuvel and Huisman's samples were 0.42, 0.50, and 0.66 dL/g [21]. As with birefringence, it appears that the greater density of the samples in this study compared to previously investigated PET fibers spun at the same speeds was due to the greater molecular weight of our samples.

Modulus

The torsional modulus (TM) of the untreated fibers rose slightly with spinning speed and to a larger extent after drawing (Table 2). The elevations are attributed to the increases in orientation induced by the processing received by the fibers.

The initial modulus (IM) of the fibers was also measured so that an estimate of the cohesive anisotropy, as given by the ratio IM/TM [14], could be calculated. For an isotropic fiber, the ratio IM/TM is between 2 and 3 [14]. The ratio increases as the fiber's axial cohesion becomes greater relative to its radial cohesion. Sample U1, with IM/TM equal to 3.05, was essentially isotropic. Augmentation of the spinning speed resulted in greater cohesive anisotropy which was further enhanced by drawing (Table 2). The effects of drawing and spinning speed come about due to the dependence of anisotropy on molecular orientation [16]. As the PET chains become more oriented, there is greater opportunity for radial interaction between the pi electrons of neighboring benzene rings. This interaction, combined with the greater orientation, increases the axial cohesion of the fiber and thus IM/TM. Birefringence can be used as a measure of optical anisotropy, and consequently should correlate with IM/TM. In fact, the relationship between IM/TM and birefringence was linear (Fig. 1). Therefore, it appears IM/TM can be predicted from birefringence determinations.

Tenacity

As expected, the tenacity of the undrawn fibers rose progressively as the spinning speed increased, since orientation and crystallinity had increased also (Table 2). The drawn fibers were stronger than their undrawn precursors, again due to their higher birefringence and crystallinity (Table 2). Orienting the polymer chains along the fiber axis results in greater strength in the axial direction. An additional factor contributing to the higher strength is that during the drawing process matter moves from the fiber interior to the fiber surface, decreasing the number of surface defects [17]. Other things being equal, strength is statistically determined by the number of defects in or on the fiber.

The tenacity of the undrawn fibers used in this study is slightly higher than that of the fibers used by Chen et al. [5] and spun at comparable speeds. Again, the difference can be attributed to the effect of molecular weight.

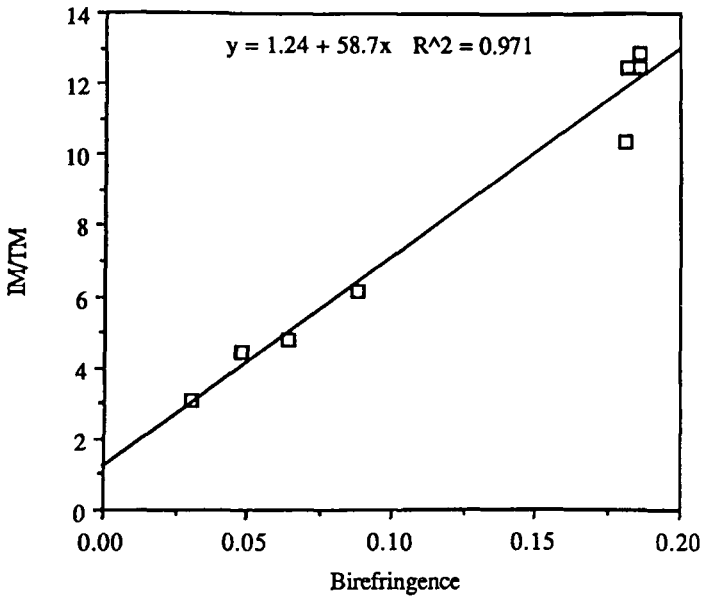

FIG. 1. Relation between IM/TM ratio and birefringence of unrelated PET fibers.

NaOH Hydrolyzed Fibers

Weight Loss

Weight loss of all samples proceeded in a linear fashion (Figs. 2 and 3), typical of aqueous NaOH hydrolysis. The rate of weight loss was determined by the fibers' fine structure. Within each sample set (undrawn and drawn), the rate of weight loss generally decreased somewhat with increasing spinning speed, as noted by the change in slope. The differences in rates are due to the various degrees of orientation and crystallinity at different spinning speeds of the starting samples (Table 2). Since untreated U1 was the least oriented and crystalline fiber, it was expected that this sample would hydrolyze the most quickly. The slope of the line for Sample U2, however, was the greatest (Fig. 2). It should be noted that at weight losses greater than 75% the data for U1 became somewhat scattered, giving it a lower R^2 value than that of the other fibers. In fact, if the data corresponding to the two highest weight losses of Sample U1 are ignored, the equation of the line is then $y = -0.900 + 5.18x$ and $R^2 = 0.990$, and the slope for U1 would indeed be greater than that of U2.

At all speeds, drawing slowed hydrolysis considerably due to the large increase in order of the polymer chains (cf. Figs. 2 and 3) even though the drawn samples were much finer than the undrawn samples (cf. tex values in Table 1). With finer fibers the available surface per unit weight would be greater and therefore the hydrolysis would be expected to proceed faster with such products. Thus, although the reaction is confined to the fiber surface, the structure of that surface affects the rate at which hydrolysis occurs. Collins et al. [9] observed similar effects in their study of conventionally spun and drawn PET fibers before and after heat setting.

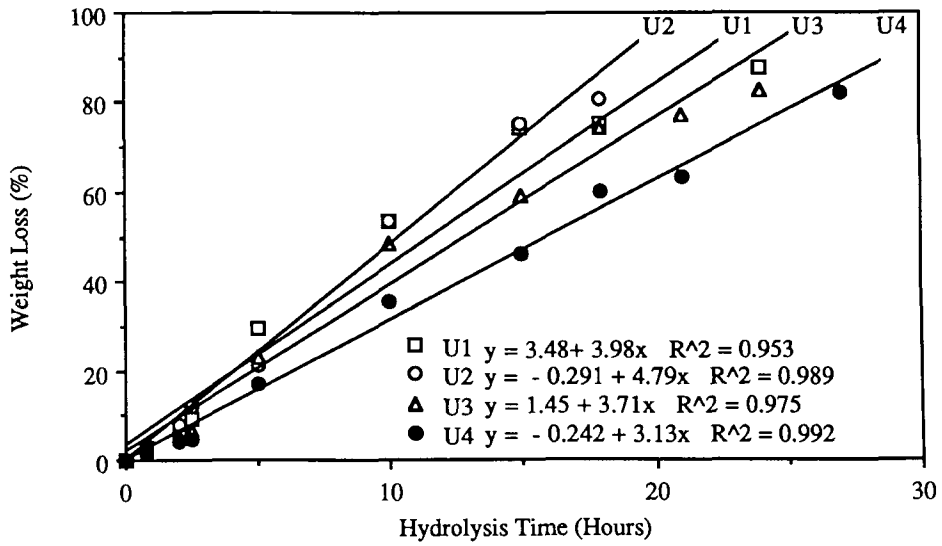

FIG. 2. Weight loss–hydrolysis time relationship for undrawn NaOH-hydrolyzed PET fibers.

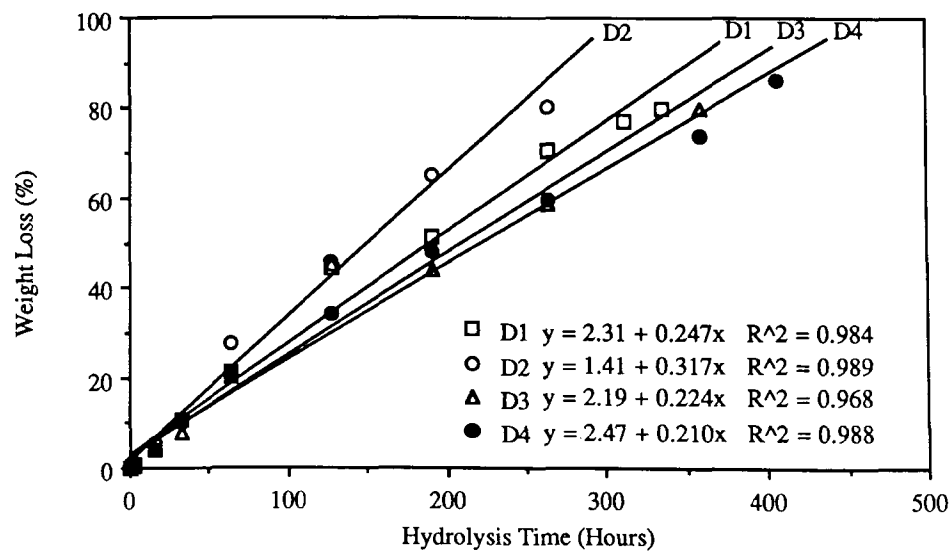

FIG. 3. Weight loss–hydrolysis time relationship of drawn NaOH-hydrolyzed PET fibers.

Scanning Electron Microscopy

Untreated PET fibers appeared round and fairly smooth (Figs. 4 and 5). The surface debris is either extraneous spin finish or oligomeric matter. Scanning electron micrographs of hydrolyzed fibers (Figs. 6 and 7) revealed pits on the fiber surface, consistent with PET containing titanium dioxide, a delusterant. The chains surrounding the TiO_2 particles are purported to be amorphous and less oriented than chains in regions farther from the particles such that preferential attack by the NaOH occurs at these unordered sites, resulting in pit formation [18]. The pits on the undrawn fibers were rounded (Fig. 6). In contrast, the drawn fibers' pits were highly elongated and oriented along the fiber axis (Fig. 7), presumably due to polymer flow around the TiO_2 particles during the drawing process. As weight loss proceeded, the pits became larger and more numerous due to the hydrolysis. It should be noted that all the micrographs shown are of Samples U1 and D1. However, essentially the same observations were made on the other samples.

Birefringence

Since the Becke line method is sensitive to orientation at the fiber surface [19] and hydrolysis reveals fresh surface with increasing weight loss, any change of orientation across the fiber radius can be detected. The birefringence of the undrawn samples spun at the two slower speeds (Samples U1 and U2) did not change significantly as the core of the fiber was approached (Fig. 8); thus, the orientation

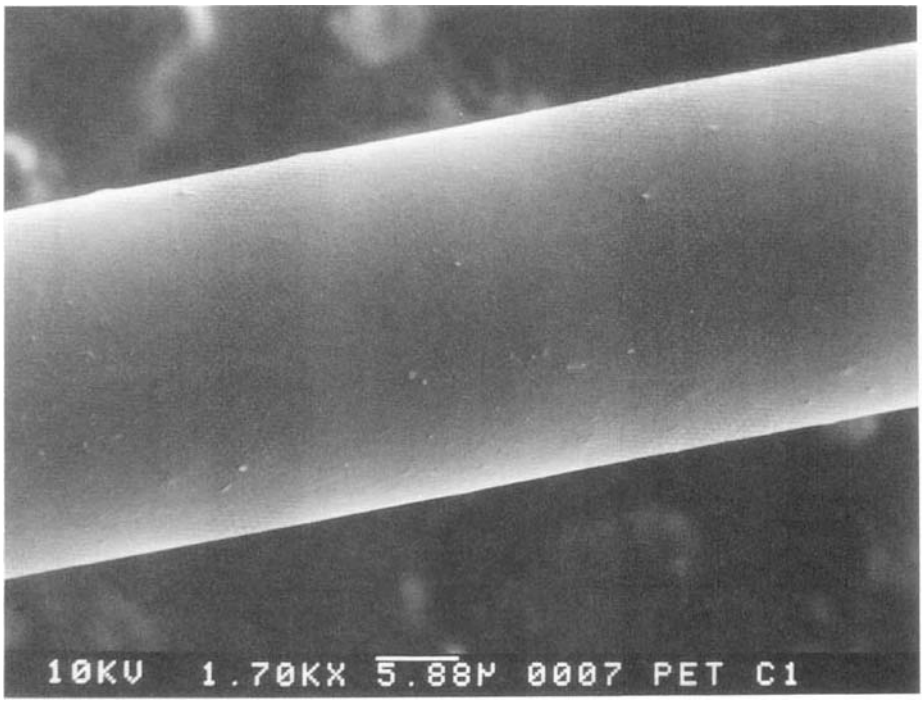

FIG. 4. Scanning electron micrograph of untreated, undrawn PET fiber U1.

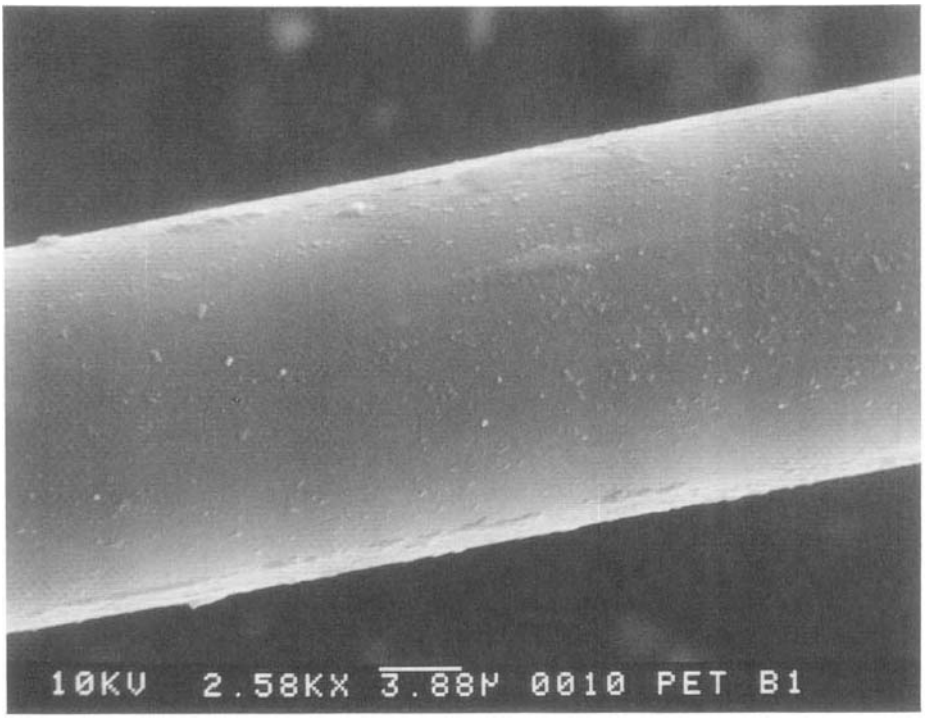

FIG. 5. Scanning electron micrograph of untreated, undrawn PET fiber D1.

of these samples was radially homogeneous. The undrawn samples spun at the two faster speeds (Samples U3 and U4) increased in birefringence at low weight loss and then fell to slightly less than the original value further into the fiber (Fig. 8), which is indicative of a layer of increased orientation just inside the original exterior. This may be due to the release of pressure in the molten polymer upon exiting the spinnerette which might allow the outside layer of the fiber to relax and become slightly less oriented. Fujimoto et al. [8] found that birefringence measured using an interference microscope is higher in the skin than in the core of PET fibers spun at high spinning speeds. A layer of lower birefringence at the very exterior of the fiber can be observed in their data, but they did not provide any explanation.

The orientation of the drawn fibers tended to decrease progressively a small but significant amount toward the fiber center (Fig. 9 and Table 3).

Density

Density of all samples remained essentially constant after removal of layers of polymer by hydrolysis (Figs. 10 and 11). Crystallinity measured by density is not sensitive to any particular portion of the fiber; rather, density is a measure of the overall molecular order. Nevertheless, the data do indicate that there were no large differences between the degree of crystallinity of the entire fiber and that of the interior after much of the fiber had been removed by hydrolysis. These results are in contrast to those found using conventionally spun and drawn PET fibers. Using

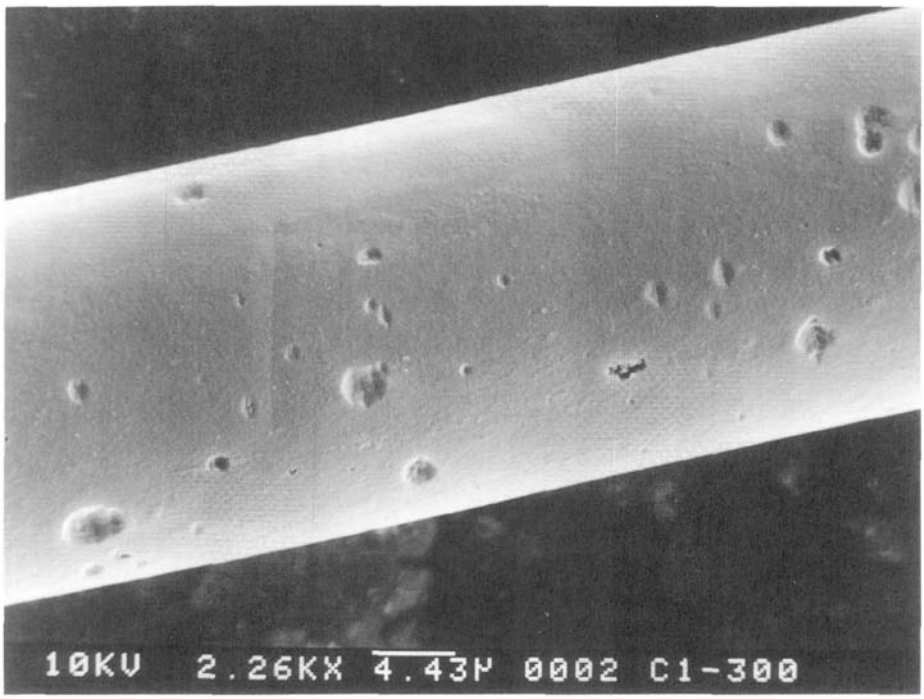

FIG. 6. Scanning electron micrograph of undrawn PET fiber U1 hydrolyzed in aqueous NaOH to a weight loss of 29.5%.

such fibers, Collins et al. [9] did find differences in degree of crystallinity across the fiber radius; density increased with hydrolysis time.

It appears that the density versus weight loss curves for undrawn Samples U3 and U4 (Fig. 10) take the same shape as the birefringence versus weight loss curves for these samples (Fig. 8). Although the changes in density of these samples were not significant, the shape of the curves may suggest that a layer of greater crystallinity might be detected with a method more sensitive to measuring intrinsic crystallinity at specific locations in the fiber. Electron diffraction patterns of PET fibers spun at 9000 m/min obtained by Mukhopadhyay and coworkers [1] revealed greater degrees of crystallinity and orientation in the fibers' skin than at the core.

Modulus

IM and TM were measured on selected hydrolyzed samples for the purpose of detecting any changes in cohesive anisotropy and, thus, molecular orientation, across the fiber radius. To measure TM, the fiber was twisted through an angle of 85°. Upon twisting a cylinder, the exterior experiences greater distortion relative to the interior [20]. TM, therefore, should be sensitive to the orientation at the fiber surface.

The TM versus weight loss curves for undrawn Samples U3 and U4 (Fig. 12) take essentially the same shape as the birefringence versus weight loss curves of

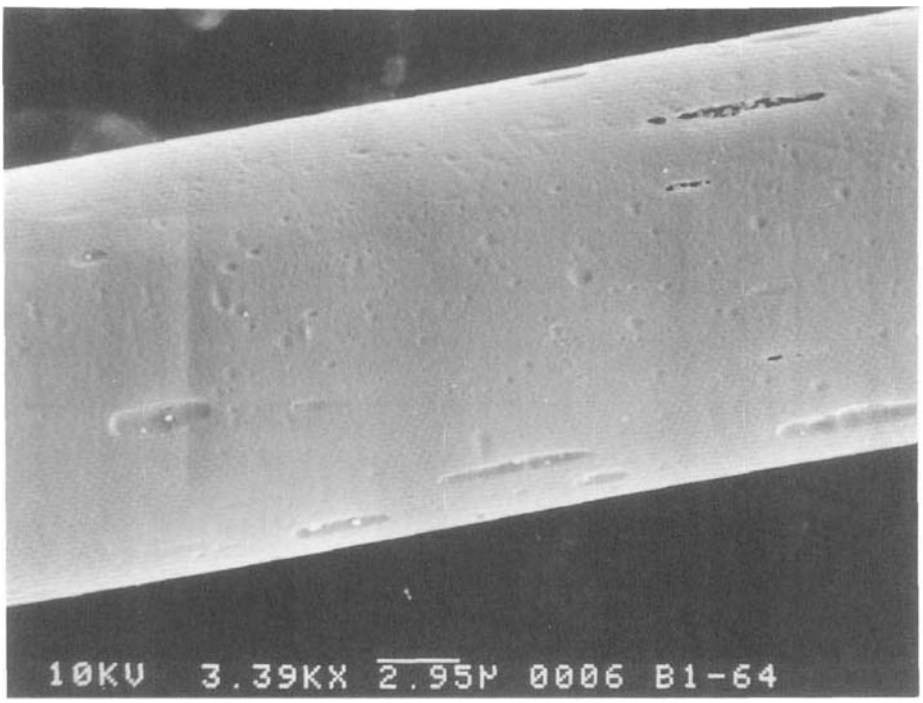

FIG. 7. Scanning electron micrograph of drawn PET fiber D1 hydrolyzed in aqueous NaOH to a weight loss of 21.4%.

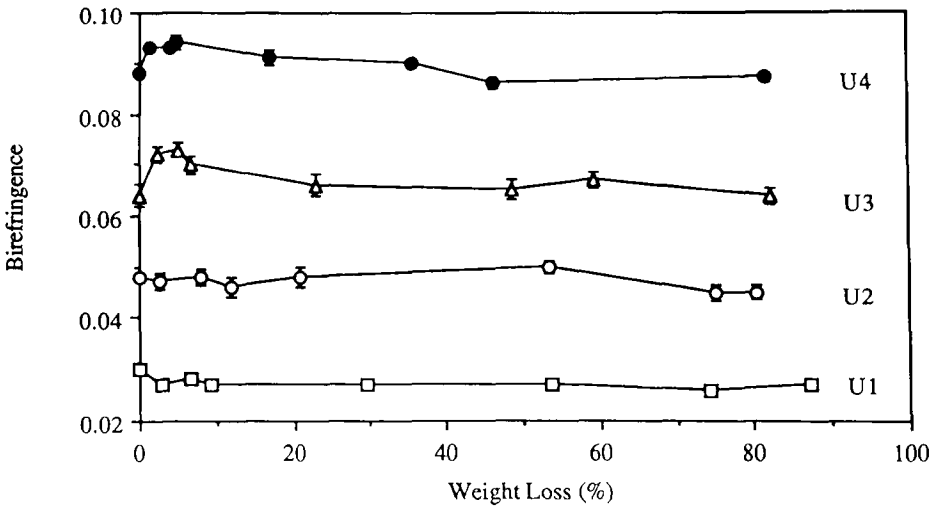

FIG. 8. Birefringence of undrawn NaOH-hydrolyzed PET fibers.

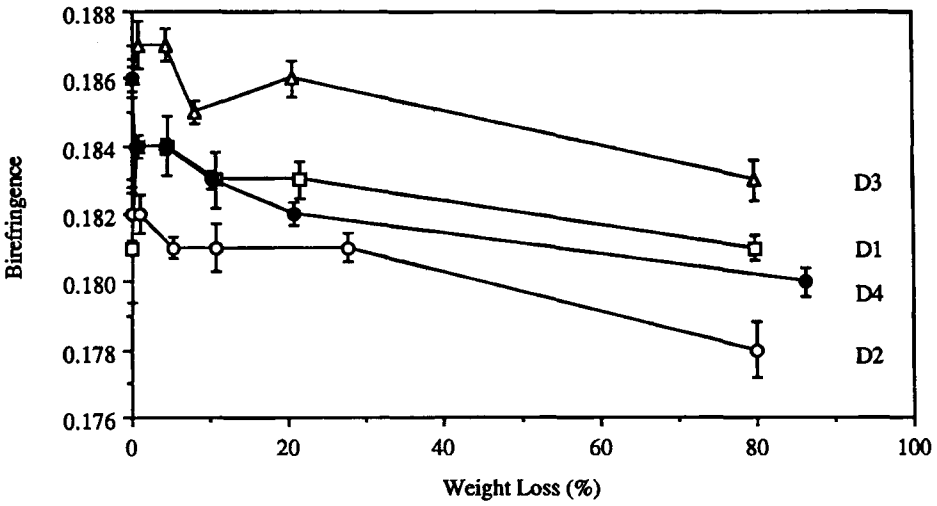

FIG. 9. Birefringence of NaOH-hydrolyzed drawn PET fibers.

these samples. That is, there is a layer of increased orientation just inside the original fiber periphery. As more of the fiber was removed by hydrolysis, TM decreased to slightly less than that of the untreated fiber. For the drawn fibers, TM was approximately constant across the fiber radius, with the exception of Sample D2 where the data were scattered (Fig. 13).

For all the samples except U1 the cohesive anisotropy of the starting fiber was higher than that of the fiber core (IM/TM of the fiber with the highest weight loss). (Tables 4 and 5). Thus the fiber core appears to be less anisotropic than the fiber skin. In fact, the IM/TM ratios of the cores of Samples U2, U3, and U4 are all less than 3, indicating that these fibers are isotropic at the core. It appeared from the birefringence measurements that the orientation of the core is only slightly less than that of the skin. This would suggest that the IM/TM ratio is a more sensitive measure of anisotropy as it pertains to physical properties than is birefringence, and that the properties of the cores of Samples U2, U3, and U4 are indeed significantly different than their peripheries in this regard.

The observed greater percent decrease in the IM/TM ratio for the undrawn fibers than for the drawn fibers as hydrolysis proceeded can be attributed to a combination of two factors. First, drawing the fibers made them more homogeneous radially, as also seen from the birefringence data. Second, the IM of the undrawn fibers decreased much more than that of the drawn fibers, causing the IM/TM ratio to also decrease more rapidly.

Tenacity

Tenacity of NaOH hydrolyzed fibers typically does not change much due to the topochemical nature of the reaction. Any decreases in tenacity which do occur may be due to the rugosity of fiber surfaces caused by pitting which provides sites where failure can be initiated [9, 18]. In this study, the undrawn samples showed greater loss in tenacity than did the drawn samples (Tables 6 and 7). Tenacity of the

TABLE 3. Birefringence of Aqueous NaOH Hydrolyzed Drawn PET Fibers

Sample	Weight loss, %	Birefringence[a]
D1	Untreated	0.181 (1.06×10^{-3})
	0.72	0.184 (3.42×10^{-4})
	4.39	0.184 (8.72×10^{-4})
	10.7	0.183 (8.06×10^{-4})
	21.4	0.183 (5.26×10^{-4})
	79.8	0.181 (3.67×10^{-4})
D2	Untreated	0.182 (7.67×10^{-4})
	0.90	0.182 (5.62×10^{-4})
	5.31	0.181 (3.00×10^{-4})
	10.7	0.181 (7.12×10^{-4})
	27.6	0.181 (4.27×10^{-4})
	80.1	0.178 (8.23×10^{-4})
D3	Untreated	0.186 (5.58×10^{-4})
	0.68	0.187 (7.15×10^{-4})
	4.20	0.187 (4.99×10^{-4})
	7.97	0.185 (3.59×10^{-4})
	20.4	0.186 (5.54×10^{-4})
	79.8	0.183 (5.93×10^{-4})
D4	Untreated	0.186 (3.79×10^{-4})
	0.56	0.184 (3.48×10^{-4})
	4.24	0.184 (2.24×10^{-4})
	10.3	0.183 (2.49×10^{-4})
	20.8	0.182 (3.14×10^{-4})
	86.4	0.180 (4.07×10^{-4})

[a]Standard errors in parentheses.

undrawn samples remained essentially constant until a weight loss of between 20 and 35% was achieved, at which point it fell to less than 77% of the untreated value. This behavior is consistent with the tensile behavior of NaOH hydrolyzed conventionally spun and drawn PET fibers [9]. In contrast to the undrawn samples, the higher levels of orientation and crystallinity combined with few defects imparted by drawing made the drawn fibers less susceptible to early fracture after hydrolysis. Even after approximately 80% weight loss, the drawn samples retained nearly 70% of their original tenacity compared to less than 50% tenacity retention at this weight loss for the undrawn fibers. The decrease in tenacity of the hydrolyzed drawn fibers at high weight losses is probably due to a combination of surface defects and a tendency toward decreasing orientation near the center of the fiber. The greater number of defects in the untreated undrawn fibers in conjunction with the pits present after hydrolysis caused a 5 to 10% tenacity loss after a relatively small weight loss. The fact that tenacity did not decrease markedly until a weight loss of 20 to 35% suggests that the distribution of defects is not homogeneous across the fiber radius; there are more defects toward the fiber center.

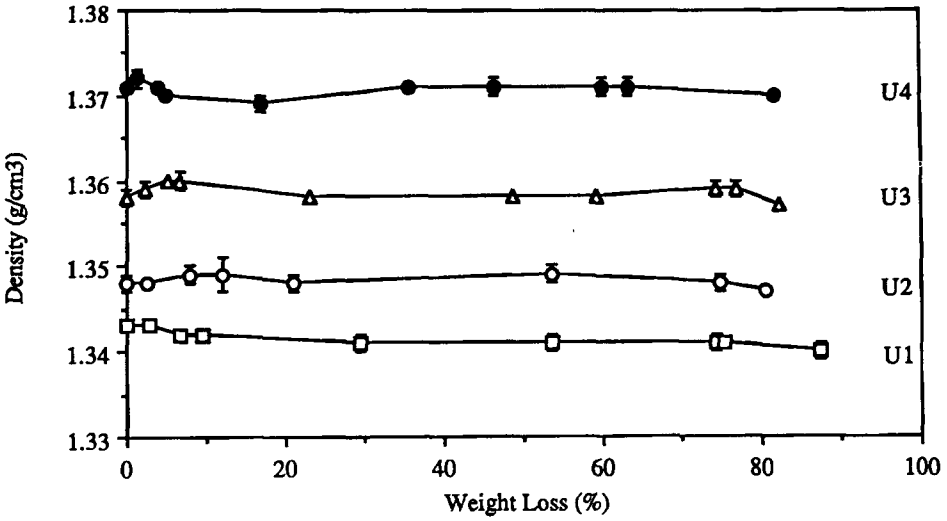

FIG. 10. Density of NaOH-hydrolyzed undrawn PET fibers.

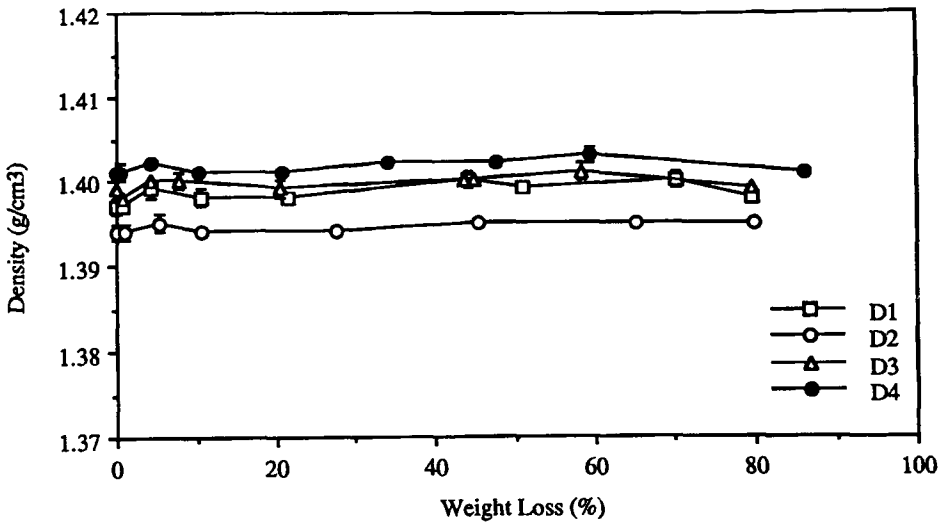

FIG. 11. Density of NaOH-hydrolyzed drawn PET fibers.

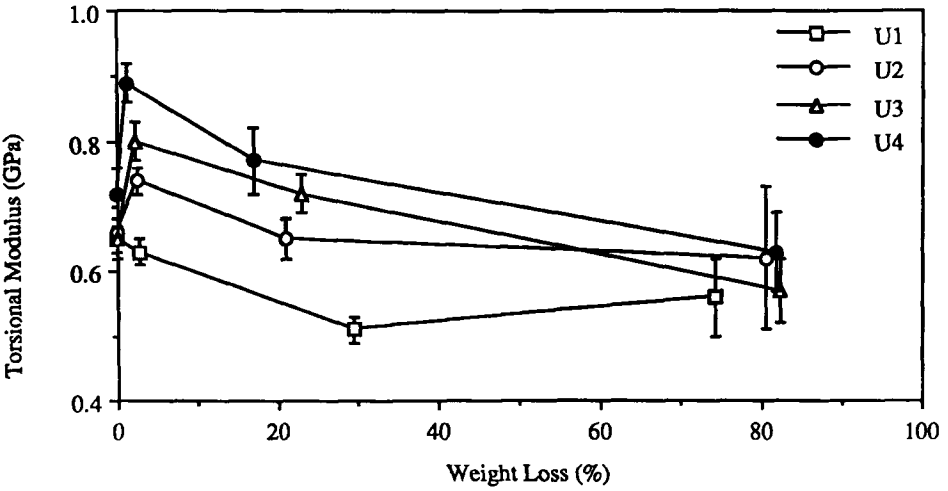

FIG. 12. Torsional modulus of NaOH-hydrolyzed undrawn PET fibers.

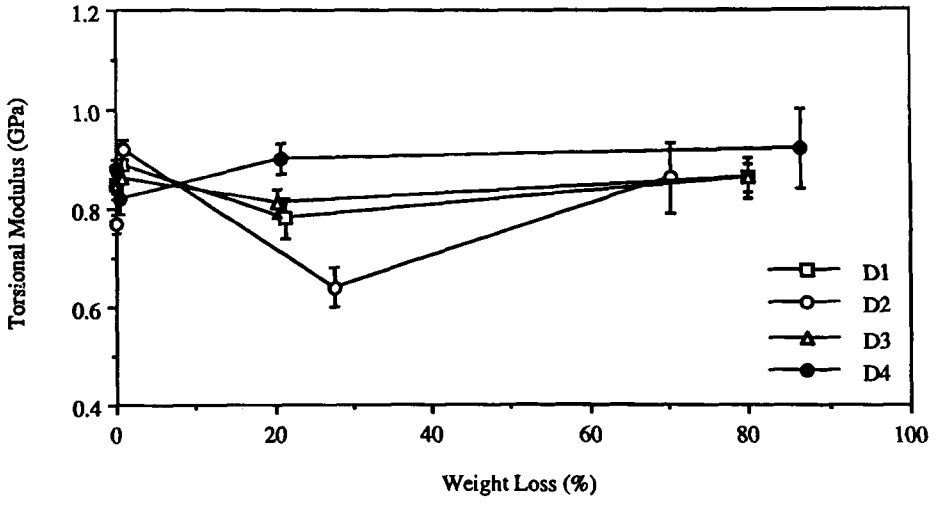

FIG. 13. Torsional modulus of NaOH-hydrolyzed drawn PET fibers.

TABLE 4. Initial and Torsional Moduli (IM and TM, respectively) of Aqueous NaOH Hydrolyzed Undrawn PET Fibers

Sample	Weight loss, %	IM,[a] GPa	TM,[a] GPa	IM/TM
U1	Untreated	1.98 (0.03)	0.65 (0.03)	3.05
	2.85	1.81 (0.04)	0.63 (0.03)	2.87
	29.5	1.95 (0.08)	0.51 (0.02)	3.82
	74.3	2.15 (0.15)	0.56 (0.06)	3.84
U2	Untreated	2.93 (0.10)	0.66 (0.02)	4.44
	2.56	3.07 (0.11)	0.74 (0.02)	4.15
	21.0	2.51 (0.08)	0.65 (0.03)	3.86
	80.5	1.05 (0.09)	0.62 (0.11)	1.69
U3	Untreated	3.10 (0.08)	0.65 (0.02)	4.77
	2.26	3.04 (0.14)	0.80 (0.03)	3.80
	23.1	2.97 (0.20)	0.72 (0.03)	4.13
	82.3	1.06 (0.07)	0.57 (0.05)	1.86
U4	Untreated	4.42 (0.16)	0.72 (0.04)	6.14
	1.37	4.36 (0.14)	0.89 (0.03)	4.90
	17.0	4.51 (0.29)	0.77 (0.05)	5.86
	81.8	1.63 (0.10)	0.63 (0.06)	2.59

[a]Standard errors in parentheses.

TABLE 5. Initial and Torsional Moduli (IM and TM, respectively) of Aqueous NaOH Hydrolyzed Drawn PET Fibers

Sample	Weight loss, %	IM,[a] GPa	TM,[a] GPa	IM/TM
D1	Untreated	8.81 (0.28)	0.85 (0.03)	10.36
	0.72	9.05 (0.30)	0.89 (0.04)	10.17
	21.4	9.18 (0.26)	0.78 (0.04)	11.77
	79.8	8.85 (0.37)	0.86 (0.03)	10.29
D2	Untreated	9.62 (0.38)	0.77 (0.02)	12.49
	0.90	9.84 (0.31)	0.92 (0.02)	10.70
	27.6	8.79 (0.12)	0.64 (0.04)	13.73
	80.1	7.86 (0.27)	0.86 (0.07)	9.14
D3	Untreated	10.61 (0.44)	0.85 (0.02)	12.48
	0.68	9.67 (0.32)	0.86 (0.04)	11.24
	20.4	10.25 (0.19)	0.81 (0.03)	12.65
	79.8	8.27 (0.42)	0.86 (0.04)	9.62
D4	Untreated	11.31 (0.37)	0.88 (0.02)	12.85
	0.56	11.57 (0.27)	0.82 (0.03)	14.11
	20.8	9.60 (0.24)	0.90 (0.03)	10.67
	86.4	8.43 (0.44)	0.92 (0.08)	9.16

[a]Standard errors in parentheses.

TABLE 6. Tenacity of Aqueous NaOH Hydrolyzed Undrawn PET Fibers

Sample	Weight loss, %	Tenacity,[a] g/tex	Relative tenacity
U1	Untreated	22.3 (0.49)	1.00
	2.85	22.8 (0.41)	1.02
	6.64	23.4 (0.30)	1.05
	9.36	23.0 (0.29)	1.03
	29.5	17.4 (0.28)	0.78
	53.6	13.5 (0.38)	0.61
	74.3	12.1 (0.41)	0.54
	75.3	8.76 (0.76)	0.39
U2	Untreated	27.7 (0.34)	1.00
	2.56	26.1 (0.35)	0.94
	7.95	25.8 (0.32)	0.93
	12.0	25.3 (0.26)	0.91
	21.0	21.2 (0.29)	0.77
	53.5	14.4 (0.57)	0.52
	75.0	11.3 (0.59)	0.41
	80.5	13.6 (0.57)	0.49
U3	Untreated	30.4 (0.35)	1.00
	2.26	28.3 (0.53)	0.93
	5.14	28.4 (0.34)	0.93
	6.63	28.1 (0.39)	0.92
	23.1	23.8 (0.31)	0.78
	48.6	20.4 (0.56)	0.67
	59.2	12.7 (0.67)	0.42
	74.4	8.28 (0.70)	0.27
	77.0	8.34 (0.77)	0.27
U4	Untreated	31.0 (0.32)	1.00
	1.37	30.6 (0.45)	0.99
	3.95	31.2 (0.49)	1.01
	4.75	30.4 (0.36)	0.98
	17.0	29.3 (0.41)	0.95
	35.7	26.5 (0.61)	0.85
	46.3	19.4 (0.35)	0.63
	60.1	21.2 (0.76)	0.68
	63.3	17.6 (0.93)	0.57
	81.8	13.5 (1.1)	0.44

[a]Standard errors in parentheses.

TABLE 7. Tenacity of Aqueous NaOH Hydrolyzed Drawn PET Fibers

Sample	Weight loss, %	Tenacity,[a] g/tex	Relative tenacity
D1	Untreated	69.1 (1.1)	1.00
	0.72	69.1 (1.2)	1.00
	4.39	69.6 (1.1)	1.01
	10.7	70.0 (1.0)	1.01
	21.4	69.6 (0.68)	1.01
	44.2	64.0 (1.2)	0.93
	51.2	61.2 (1.3)	0.89
	70.3	58.8 (1.2)	0.85
	79.8	58.4 (1.8)	0.85
D2	Untreated	73.6 (1.3)	1.00
	0.90	73.9 (0.73)	1.00
	5.31	72.7 (0.64)	0.99
	10.7	68.4 (0.86)	0.93
	27.6	68.5 (0.94)	0.93
	45.5	64.5 (1.0)	0.88
	65.2	54.6 (1.1)	0.74
	80.1	50.7 (1.5)	0.69
D3	Untreated	78.3 (1.3)	1.00
	0.68	74.6 (0.74)	0.95
	4.20	75.0 (0.68)	0.96
	7.97	75.3 (1.1)	0.96
	20.4	74.6 (0.64)	0.95
	43.7	66.0 (0.90)	0.84
	58.6	69.2 (0.79)	0.88
	79.8	54.1 (1.7)	0.69
D4	Untreated	78.1 (0.55)	1.00
	0.56	77.6 (0.54)	0.99
	4.24	72.0 (0.77)	0.92
	10.3	72.8 (0.93)	0.93
	20.8	65.5 (1.2)	0.84
	34.3	68.8 (1.2)	0.88
	47.8	63.7 (1.3)	0.82
	59.5	63.2 (1.2)	0.81
	86.4	52.5 (2.5)	0.67

[a]Standard errors in parentheses.

CONCLUSIONS

The relatively high molecular weight of the PET used in this study yields undrawn samples of higher orientation and crystallinity than those obtained by workers using PET of lower molecular weight but spun at similar speeds. As expected, increasing the spinning speed and subsequently drawing results in greater levels of orientation and crystallinity in the product. Considering the undrawn and

drawn fibers together, a linear relationship between cohesive and optical anisotropy can be obtained. In terms of orientation, the undrawn high-speed spun PET fibers exhibit some skin–core type of structure, depending on spinning speed, whereas their drawn counterparts appear to be radially homogeneous, indicating that they do not have a skin. The undrawn fibers, again depending on spinning speed, might differ in crystallinity from the exterior to the interior if a more sensitive measure of crystallinity than density measurements can be applied. In the drawn samples, generally, a small but significant decrease in birefringence is observed as the center of the fiber is approached. The drawing process appears to produce fibers without a skin–core structure and less susceptible to tenacity loss due to surface defects.

ACKNOWLEDGMENT

The authors thank Hoechst-Celanese Corporation for supplying the fibers and for financial support.

REFERENCES

[1] S. K. Mukhopadhyay, E. M. O. Bebbington, and P. W. Foster, *Text. Res. J.*, *62*, 403 (1992).
[2] J. Shimizu, N. Okui, and T. Kikutani, *Sen-i Gakkaishi*, *37*, T-135 (1981).
[3] G. Vassilatos, B. H. Knox, and H. R. E. Frankfort, in *High-Speed Fiber Spinning: Science and Engineering Aspects* (A. Ziabicki and H. Kawai, Eds.), Wiley, New York, 1985, Chap. 14.
[4] V. B. Gupta, S. K. Sett, and D. D. Deorukhkar, *Polym. Commun.*, *30*, 341 (1989).
[5] G.-Y. Chen, J. A. Cuculo, and P. A. Tucker, *J. Appl. Polym. Sci.*, *44*, 447 (1992).
[6] J. Shimizu, N. Okui, T. Kikutani, and K. Toriumi, *Sen-i Gakkaishi*, *34*, T-93 (1978).
[7] H. M. Heuvel and R. Huisman, in *High-Speed Fiber Spinning: Science and Engineering Aspects* (A. Ziabicki and H. Kawai, Eds.), Wiley, New York, 1985, Chap. 11.
[8] K. Fujimoto, K. Iohara, S. Ohwaki, and Y. Murase, *J. Appl. Polym. Sci.*, *42*, 1509 (1991).
[9] M. J. Collins, S. H. Zeronian, and M. Semmelmeyer, *Ibid.*, *42*, 2149 (1991).
[10] (a) S. H. Zeronian and M. J. Collins, *Text. Prog.*, *20*(2), 1 (1989). (b) M. J. Collins, S. H. Zeronian, and M. L. Marshall, *J. Macromol. Sci–Chem.*, *A28*(8), 775 (1991). (c) N. Kallay, A. M. Grancarić, and M. Tomić, *Text. Res. J.*, *60*, 663 (1990).
[11] F. W. Billmeyer, *J. Polym. Sci.*, *4*, 83 (1949).
[12] F. Rodriguez, *Principles of Polymer Systems*, Hemisphere, Washington, D.C., 1982, Chap. 7.
[13] S. Berkowitz, *J. Appl. Polym. Sci.*, *29*, 4353 (1984).
[14] R. Meredith, *J. Text. Inst.*, *45*, T489 (1954).

[15] E. L. Ringwald and E. L. Lawton, in *Polymer Handbook* (J. Brandrup and E. H. Immergut, Eds.), Wiley, New York, 1975, p. V-72.
[16] D. W. Hadley, P. R. Pinnock, and I. M. Ward, *J. Mater. Sci.*, *4*, 152 (1969).
[17] A. R. Bunsell, in *Fibre Reinforcements for Composite Materials* (A. R. Bunsell, Ed.), Elsevier, Amsterdam, 1988, Chap. 1.
[18] C. M. Solbrig and S. K. Obendorf, *Text. Res. J.*, *61*, 177 (1991).
[19] J. L. Stoves, *Fibre Microscopy*, Van Nostrand, Princeton, New Jersey, 1958, p. 59.
[20] D. Q. Fletcher, *Mechanics of Materials*, Holt, Rinehart, and Winston, New York, 1985, Chap. 6.
[21] S. A. Holmes, "Studies of High-Speed Spun Poly(Ethylene Terephthalate) Fibers," Ph.D. Thesis, University of California, Davis, 1993.

Received October 19, 1993
Revision received January 14, 1994